Friction Behavior of Boric Acid and Annealed Boron Carbide Coatings Studied by In Situ Raman Tribometry©

S. D. DVORAK
University of Maine
Orono, Maine 04469-5711
and
K. J. WAHL (Member, STLE) AND I. L. SINGER
U.S. Naval Research Laboratory, Code 6176
Washington DC 20375-5342

Editor's Note: Opportunity Knocks, once..twice..are you listening?

Dear Industrial Tribologists:

Several years ago, Dr. Ali Erdemir, a colleague at Argonne National Labs, discovered that boric acid, an old-fashioned eye wash, is also a great solid lubricant. He based this discovery on good exploratory friction and wear testing and published the results here in *Lubrication Engineering* and elsewhere. Now the authors of this paper from the Naval Research Lab have confirmed the lubricating properties of boric acid. In addition to being a good lubricant, boric acid is environmentally safe and could be an excellent assembly/manufacturing lubricant. The last time I checked with Dr. Erdemir, he told me that boric acid still hadn't been picked up by industry and put to use. I think that's a shame. Ali's early papers were opportunity knocking once. Dr. Dvorak's paper reprinted from the July issue of *Tribology Transactions* here is opportunity knocking again…are you listening?

CDC

The sliding friction behavior of boric acid and annealed boron carbide coatings has been investigated by in situ Raman tribometry. Reciprocating sliding tests were performed in air (~20% relative humidity) at 1 mm/s with a transparent sapphire hemisphere dead weight loaded against the coated substrates. A homebuilt micro-Raman tribometer recorded the friction force as well as allowed both visualization and Raman spectroscopy of the contacts during sliding. Friction coefficients for the boric acid films remained low ($\mu \sim 0.06$) throughout sliding until failure ($\mu \sim 0.7$), at which time boric acid was lost from the contact and substrate material (aluminum) transferred to the slider. Friction coefficients for the annealed boron carbide, known to form boric acid surface films upon cooling, were initially low (0.08), then gradually increased and leveled out at about 0.2. Raman spectroscopy revealed a mixture of boric acid and carbon initially; but as the friction coefficient rose, the boric acid intensity decreased to zero while the carbon intensity increased. Correlations between friction coefficients and amounts of solid lubricating material in the contact are presented, and the role of third bodies in controlling friction is discussed.

KEY WORDS

Raman Spectroscopy; Friction Coefficient; Carbide Coatings

Final manuscript approved March 13, 2002
Review led by Robert Fusaro

INTRODUCTION

In most sliding situations, the friction coefficient for a pair of materials is not constant; instead it depends on a variety of influences including environment, contact conditions as well as material properties. Even when all the above are held fixed, the friction coefficient often evolves from run-in to one or more steady-state regimes, with or without fluctuations, prior to failure *(5)*. There are many reasons why the friction coefficient varies, and perhaps the most general reason is that the material within the sliding contact itself is changing. This material, known today as the "third body," affects friction by establishing how and where the velocity is accommodated at the sliding interface *(18)*.

Most of the knowledge correlating friction and third body effects has come from inferences derived from *ex situ* studies after worn surfaces have been separated *(6)*, *(8)*. While these inferences are valuable, one needs *in situ* chemical or optical probing of the sliding contact to confirm with certainty what processes and chemistries are controlling friction. Furthermore it is difficult, if not impossible, to determine the contact dynamics and velocity accommodation modes through *ex situ* analyses. Real-time probes have provided considerable insight into mechanical and chemical processes in the sliding interface (e.g. frictional heating through infrared and thermocouple techniques *(24)*, contact resistance *(1)*, *(35)*, optical interferometry *(20)*, *(9)*, and Fourier Transform Infrared (FTIR) *(30)* and Raman *(10)* spectroscopies). However, only through optical techniques have third body buildup, debris mobility, and velocity accommodation modes been viewed and confirmed *(34)*, *(2)*, *(23)*, *(12)*.

TABLE 1—FRICTION COEFFICIENTS OF REFERENCE MATERIAL COMBINATIONS	
MATERIAL COMBINATION	FRICTION
Sapphire/Polished Inconel	$0.6 < \mu < 0.8$
Sapphire/Un-Annealed B_4C Coating	$0.30 < \mu < 0.35$
Sapphire/Polished B_4C	$0.8 < \mu < 1.0$
Sapphire/Carbon	$0.16 < \mu < 0.20$

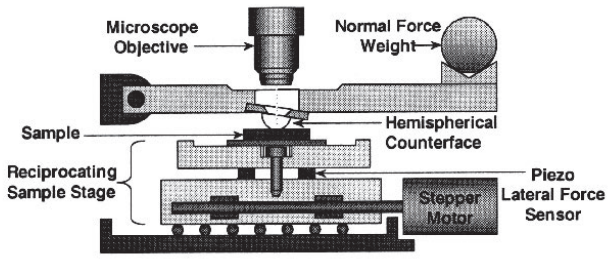

Fig. 1—*In situ* Raman tribometer schematic. Either micro-Raman spectroscopy or optical microscopy of the sliding contact can be performed through an objective aperture above the transparent hemisphere.

How third bodies affect behavior of low friction coatings has been the subject of many papers in the past decade or so *(19)*, *(3)*, *(33)*. The present study investigates the influence of third bodies on the friction behavior of boric acid and annealed boron carbide coatings. Previously, Erdemir and co-workers have demonstrated that annealed boron carbide coatings, after exposure to moisture, formed surface films of boric acid *(14), (16)*. These films gave the same low friction coefficients as boric acid. The objective of this study is to identify the third bodies generated with these coatings and correlate them with friction evolution. Real time *in situ* Raman and optical microscopy were used to identify the third bodies present in the sliding contact. In this article, the term *in situ* indicates that the analysis was performed while the two sliding surfaces were in contact, whereas *ex situ* indicates that the analysis was performed after the two surfaces were separated. The authors also address the following questions: Can the friction coefficient be predicted and quantified based on third-body coverage or composition, and are the third bodies detected *in situ* the same as the ones observed *ex situ*?

EXPERIMENTAL

Two coated samples were examined: boric acid on aluminum, and annealed boron carbide on inconel. The boric acid coating was formed by applying a boric acid solution to the surface of an aluminum 6061 substrate and allowing it to dry. The boron carbide coating was deposited on Inconel X-750 by rf-magnetron-sputtering and then annealed in air at 800°C for about 15 min. Further details of sample preparation are given elsewhere *(17)*.

Sliding experiments were performed in a home-built Raman tribometer shown in Fig. 1. The tribometer was placed beneath the 10x objective (0.3 NA) of an optical microscope, which was attached to a Raman microprobe. The microprobe consists of a low-power (25 mW) argon ion laser (514.5 nm), and a holographic spectrometer. It has a spot size of 2 μm and a spectrometer resolution of 1 cm-1. The laser beam was focused onto the coating surface, after passing through a stationary, optically-transparent hemisphere, which also served as a counterface for friction testing. The hemisphere was mounted on a lever arm loaded with dead weights. The friction force was measured with a piezo sensor housed in a stage that held the coated samples. Both average and spatially resolved friction data were recorded in a manner similar to that previously described by Belin and co-workers *(1)*, *(35)*. Only the average friction coefficient, μ = (friction force)/(normal load) averaged over each cycle, will be reported here.

Reciprocating sliding tests were performed on each of the coated samples, as well as on reference samples of carbon, (pre-annealed) boron carbide coated inconel, uncoated bulk samples of polished boron carbide and inconel. Five tests were performed on the boric acid coating and six tests on the annealed boron carbide coating. The number of cycles in a test ranged from 20 to 1200. Some tests were stopped when the friction coefficient rose rapidly to above 0.7 or severe wear was detected visually; both conditions will be designated as coating failure in this work. All tests were run at a load of 6.4 N with a sliding speed of 1 mm/s, in ambient (~20% relative humidity) air at room temperature. The counterface was a 6.35 mm diameter sapphire hemisphere, resulting in mean initial Hertzian stresses of 0.53 GPa and 0.82 GPa against aluminum and inconel, respectively. The friction coefficients for the four reference samples are given in Table 1. *In situ* microscopy was performed during friction testing, either to observe the sliding contact optically or to perform micro-Raman spectroscopy. Raman spectra were acquired from the center of the contact (unless stated otherwise) over 5 to 10 sliding cycles. Observations were recorded onto VHS tape at 30 frames/s, and still images were obtained from the videotape using a video capture card.

After the friction tests were stopped, the contacts were separated and *ex situ* Raman spectra were taken in the wear scars on hemispheres and coatings. X-Ray photoelectron spectroscopy (XPS) and stylus profilometry were also performed on some of the wear scars. XPS spectra were acquired using a monochromatic Al K-alpha source operated at 300 W (15 kV, 20 mA) and spot size of 300 μm. Analyzer pass energies of 100 eV and 20 eV were used to collect survey and high resolution spectra, respectively, and charge neutralization was accomplished with a low energy (4-5 eV) electron flood gun. Binding energies were referenced by setting the C 1s peak to 284.6 eV. Finally, Raman reference spectra for sapphire, boric acid, and boron carbide were obtained for comparison to the *in situ* results; the reference spectra are shown in Fig. 2.

RESULTS

Boric Acid Coating on Aluminum

The five tests performed on the boric acid coating showed similar friction behavior and *in situ* features. Figure 3 shows a typical friction coefficient *vs*. cycles curve. The friction coefficient started out at about 0.06, remained less than 0.1 until cycle 218, where a friction spike above 0.1 was observed. The friction coefficient recovered to $\mu < 0.1$ for 10 cycles, then increased rapidly to about 0.8. The spatially resolved friction data (not shown), displayed uniform friction along the track, even during the friction spikes and at failure.

(Continued on next page)

(Continued from previous page)

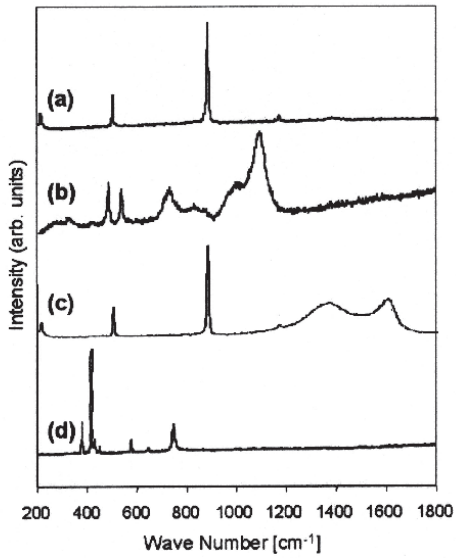

Fig. 2—Reference Raman spectra.
(a) boric acid
(b) boron carbide
(c) annealed boron carbide coating
(d) sapphire

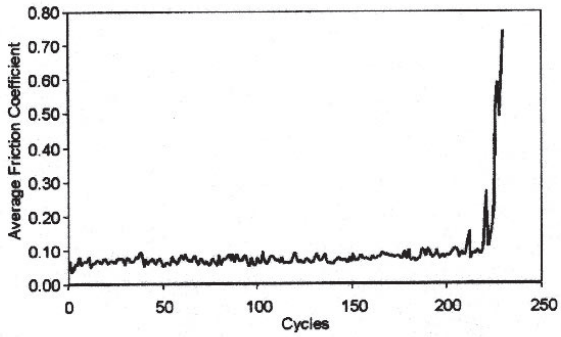

Fig. 3—Friction coefficient of sapphire ball sliding against boric acid coating on aluminum.

Figure 4 shows three *in situ* images of the interface taken during this friction test. Figure 4(a) (cycle 160) is representative of the contact as it appeared during the low-friction portion of the test. The circular area in the center of the figure, outlined by a dashed line, encompasses the apparent area of contact between the hemisphere and the wear track (area between dotted lines) on the substrate. Several dark spots can be seen inside the contact region. During sliding, these spots moved across the contact at the sliding speed, indicating that they were high spots (asperities) on the coating making contact with the hemisphere. (Spots where the hemisphere is in contact with the coating generally show up dark in a reflecting light microscope because of optical interference, as seen in the zeroth order Newton's rings between a ball and a glass plate.) Outside the contact area, fine debris particles adhered to the hemisphere.

Figure 4(b) shows an image taken at cycle 218, after the first friction spike. A bright patch can be seen in the contact zone. Videotapes showed that the patch was stationary, i.e., attached to the hemisphere; being opaque, this patch prevented visual and Raman analysis of the underlying sliding interface. The horizontal dark bands to the left and right of the bright patch show a scratch in the wear track (confirmed *ex situ* by interferometry). When the friction coefficient dropped to $\mu < 0.1$, the patch and the scratch were still visible. Figure 4(c) shows the same area during the next friction spike (cycle 228), at a friction coefficient of $\mu = 0.6$. Here the bright patch covered the entire contact area. Figure 5 shows a plot of the friction coefficient *vs.* the area fraction occupied by the bright patch. The area data were computed from images like those in Fig. 4. The dashed line is based on a simple model that will be presented in the discussion.

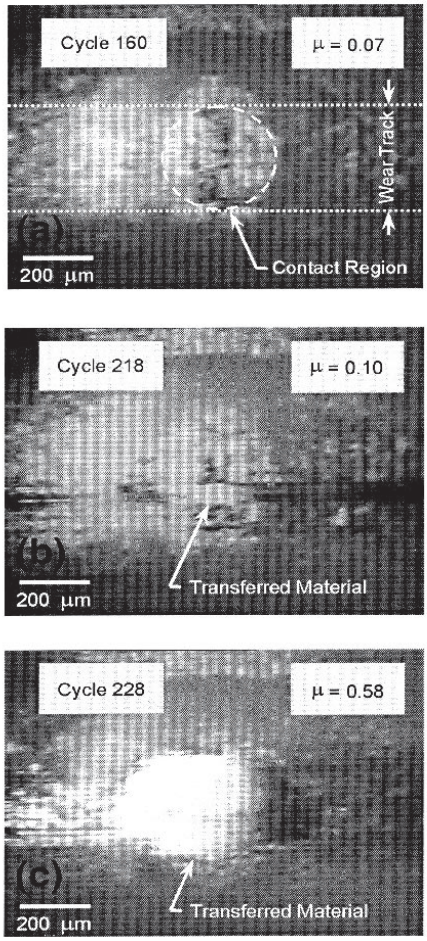

Fig. 4—Optical micrograph of the sliding contact, through the sapphire hemisphere, against boric acid coating.
(a) 160
(b) 218
(c) 228 cycles

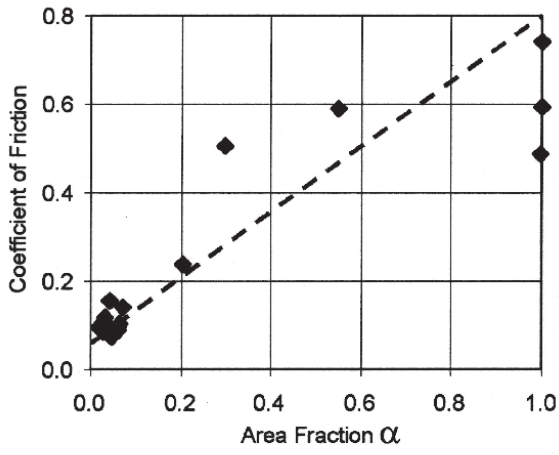

Fig. 5—Friction coefficient *vs.* area fraction for cycles 207-229.

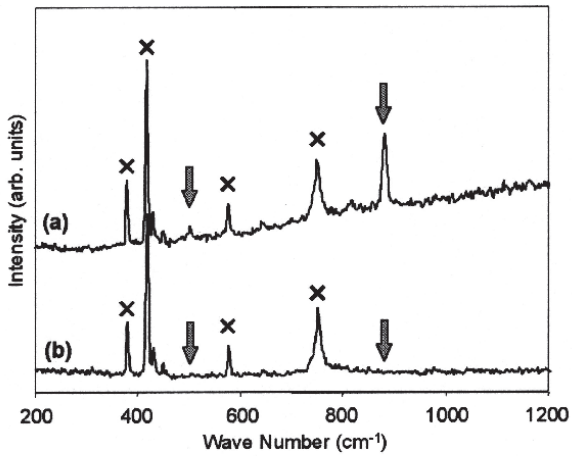

Fig. 6—*In situ* Raman spectra of contact during friction test with boric acid coatings.
(a) spectrum of intact boric acid coating
(b) spectrum of transfer film

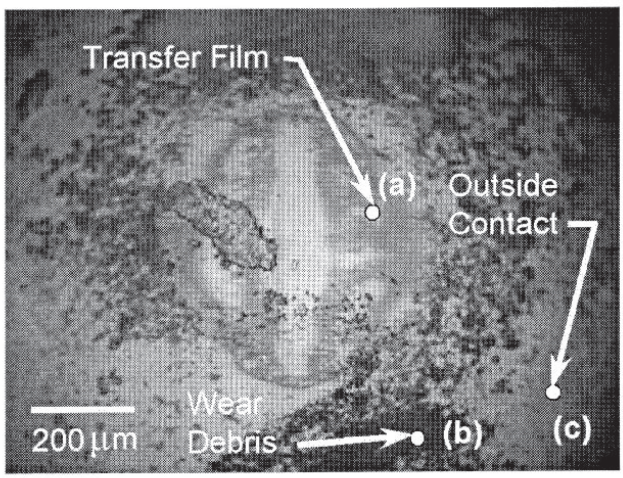

Fig. 7—Micrograph of wear scar on the sapphire hemisphere of a test interrupted after 100 cycles.
(a) buildup of transfer film
(b) wear debris
(c) unworn area of hemisphere

Figure 6 shows two *in situ* Raman spectra taken at the center of the contact area before and after the first friction spike. Spectrum (a), taken while friction was low (cycles 161-164), shows two sets of peaks: the four marked by X's are from the sapphire, and the two indicated by arrows are from boric acid (see Fig. 2). Spectrum (b) was taken on the small bright patch in the contact (shown in Fig. 4(b)) after the first significant friction spike appeared (cycles 218-224). No boric acid was detected, only the background sapphire was observed. However, boric acid peaks were seen (but not shown) in the contact area surrounding the small bright patch shown in Fig. 4(b).

Ex situ optical microscopy, Raman and XPS were performed on the wears scars of both counterfaces from the same test (in Fig. 3). The contact area on the hemisphere had a patch of shiny material, and the wear track had a deep scratch. Raman analysis on the patch and in the scratch of the wear track was unable to detect boric acid.

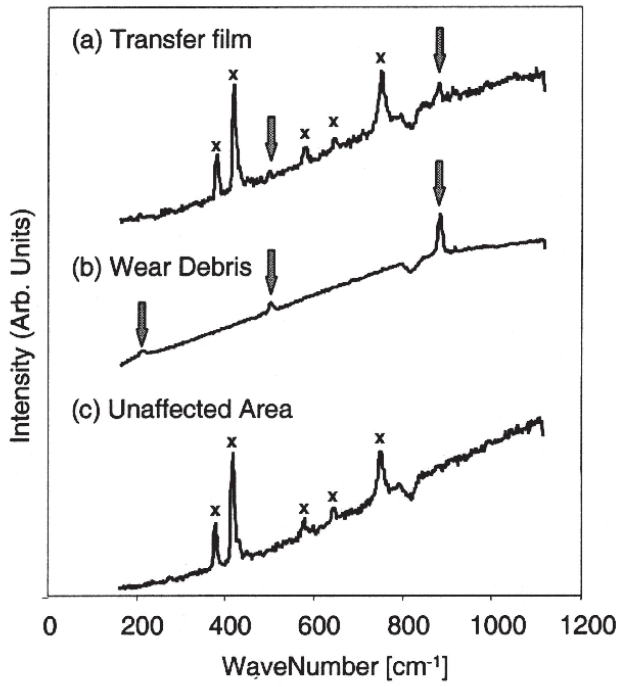

Fig. 8—*Ex situ* Raman spectra obtained at the specific location shown on Fig. 7.
(a) the transfer film
(b) loose wear debris
(c) unworn area of the hemisphere
Arrows show boric acid peaks, x's show sapphire peaks.

XPS of the patch, following charge correction, revealed peaks at 74.2 and 72.1 eV. The peaks can be assigned to oxidized and metallic aluminum; the latter confirms that the patch contained metallic aluminum transferred from the aluminum substrate.

Figure 7 shows an *ex situ* image of the wear scar on a hemisphere from a 100 cycle test stopped when the friction coefficient was still low ($\mu = 0.07$). A compact transfer film had formed in the center of the contact area, surrounded by loose wear debris. Raman spectra from the three spots in Fig. 7 are shown in Fig. 8. Boric acid was detected on the transfer film and the wear debris, but not outside the wear area. *Ex situ* Raman analysis also showed boric acid on similar low friction wear tracks. Hence, both *ex situ* and *in situ* Raman data agreed that boric acid was present on both counterfaces during low friction sliding.

Annealed Boron Carbide Coating on Inconel

The six tests performed on the annealed boron carbide coating showed similar friction behavior and *in situ* features. Figure 9 shows a typical friction coefficient *vs*. cycles curve. The friction coefficient started out at $\mu = 0.08$, slightly higher than the initial value with the boric acid coating, and climbed steadily over 400 cycles to about 0.1. From cycle 450 to 800, the friction coefficient rose from 0.1 to above 0.2, after which it dropped to a steady value of about 0.2. A similar test of sapphire against uncoated inconel gave much higher friction coefficients, between 0.6 and 0.8 (see Table 1).

Figure 10 shows three *in situ* images of the interface obtained during this test. Figure 10(a) was taken at cycle 100, during low friction sliding. The contact area appeared smoother than that in

(Continued on next page)

(Continued from previous page)

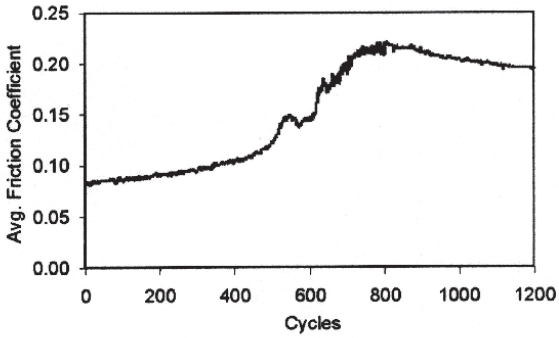

Fig. 9—Friction trace of sapphire hemisphere sliding against annealed B_4C coating on inconel.

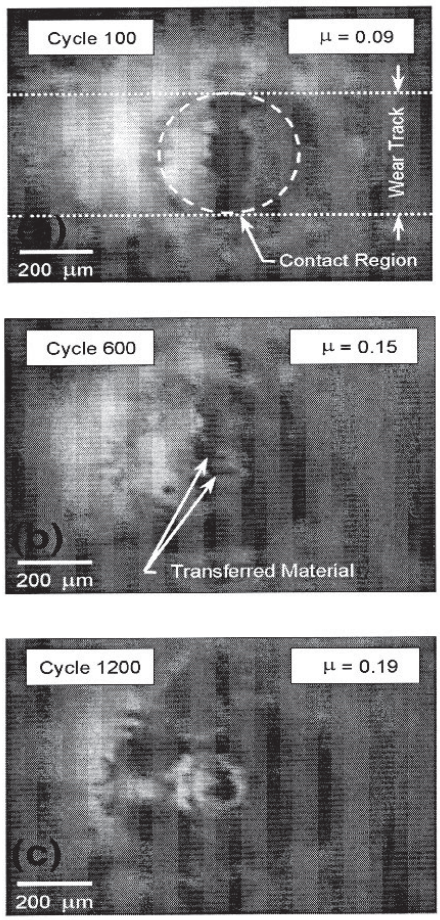

Fig. 10—View of contact in annealed B_4C coating friction test.
(a) 100
(b) 600
(c) 1200 cycles

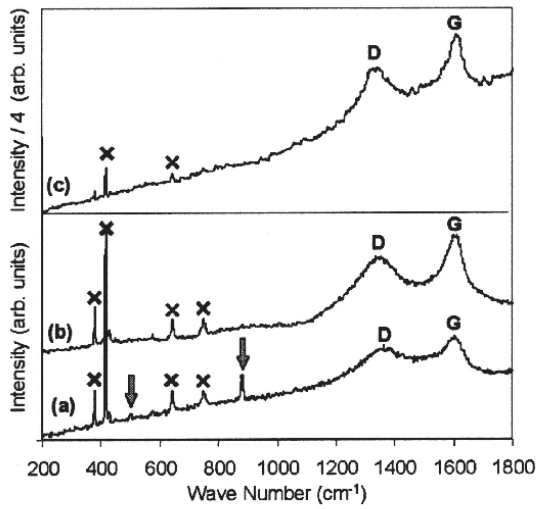

Fig. 11—*In situ* Raman of contact during sliding test of sapphire against annealed B_4C coating (see Fig. 9), showing spectra obtained.
(a) 100-108 cycles
(b) 553-562 cycles
(c) 1167-1176 cycles
Arrows show boric acid peaks, x's show sapphire peaks.
Carbon peaks are indicated by "D" and "G."

Fig. 4(a). The dark oval inside the contact area, extending the width of the wear track on the substrate, moved across the contact at the sliding speed; as before, the dark (interference) oval represents the area of the hemisphere in contact with the coating. As in the case of the boric acid coating, no buildup of material in the contact zone could be observed during low-friction sliding, $\mu < 0.1$. As the friction coefficient rose above 0.1, dark material appeared in the contact zone, as seen in Fig. 10(b), an image taken at $\mu \sim 0.15$. Video analysis showed the dark material to be a combination of loose debris moving around in the contact zone and fixed patches of transfer film adhering to the hemisphere in the center of the contact zone. Figure 10(c) shows an image of the contact taken at the end of the test, at a friction coefficient of about 0.2. The stationary dark material in the contact zone in Fig. 10(b) was no longer visible; the moving dark spots (optical interference spots) in the contact zone were similar to those observed during low-friction sliding (Fig. 10(a)). Moreover, a significant amount of debris accumulated outside the contact zone.

An *in situ* Raman spectrum obtained during low-friction ($\mu <$ 0.10) sliding is shown in Fig. 11 and marked (a). In addition to the boric acid and sapphire peaks, D and G peaks of carbon are present. The latter peaks are obtained from many types of carbon with nanoscale or amorphous structures, including graphitic and amorphous carbon *(22)*, glassy carbon and pyrolytic graphite *(29)*, *(28)*, and hydrogenated carbon *(25)*. Spectrum (b), taken at $\mu \sim 0.15$, shows that the carbon peaks became more pronounced, while the boric acid peaks disappeared. Spectrum (c), taken at $\mu \sim 0.2$, also shows much larger carbon intensities, but, again, no boric acid; note that the vertical scale of the upper spectrum has been reduced by a factor of four due to the presence of a fluorescent background.

Fifteen sets of *in situ* Raman spectra, taken during the test reported in Fig. 9, were analyzed by applying a background correction and normalizing the 881 cm-1 boric acid and carbon peak heights with respect to the dominant sapphire peak (418 cm-1). Results of this analysis are shown in Fig. 12. The height of the boric acid peak gradually decreased during the low friction ($\mu \sim 0.1$) stage of the test, disappearing around cycle 500. The D and G carbon peak heights changed very little during this stage of the test. After cycle 500, as the friction coefficient rose, the heights of the two carbon peaks increased dramatically.

Ex situ Raman spectra from the hemisphere wear scar are shown in Fig. 13. The light circular area in the center of the image was the contact area during the last cycle of the test. Raman spectrum (a) showed that it contained a large amount of carbon, whereas a spot

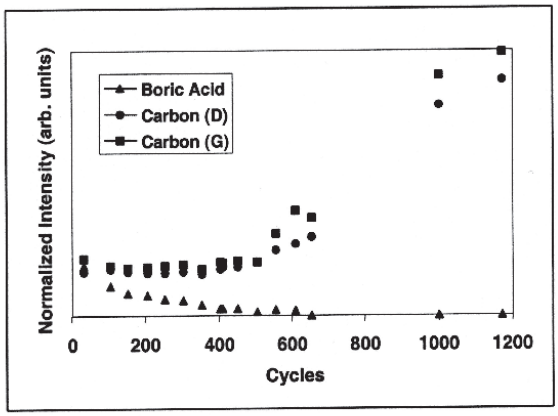

Fig. 12—Raman peak intensity of boric acid and carbon (normalized by the sapphire intensity) for the test shown in Fig. 9.

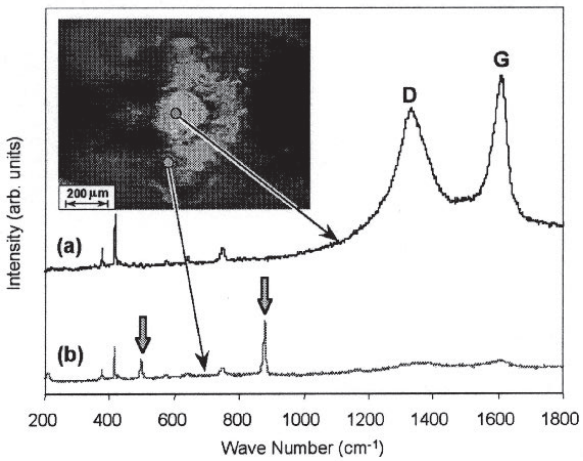

Fig. 13—*Ex situ* analysis of ball scar from test against annealed B_4C coating, showing Raman spectra.
(a) inside the contact region
(b) outside the contact region

outside the contact zone (b) still contained boric acid and much smaller carbon peaks. An *ex situ* image and corresponding Raman spectra of the wear track in the coating are shown in Fig. 14. The light horizontal area across the middle of the image runs along the center of the wear track. Raman spectrum (a) showed only carbon in the center of the wear track, but boric acid and carbon outside of the track (b). Clearly, when the friction coefficient leveled off at $\mu \sim 0.20$, the composition of the interface had changed from boric acid + carbon to carbon alone.

DISCUSSION

In the present study, two third body effects that controlled friction have been identified by *in situ* as well as *ex situ* analysis. First, with the annealed boron carbide coatings, when boric acid was at the sliding interface, the friction coefficient was low ($\mu < 0.1$); when carbon was at the interface, the friction coefficient was higher ($\mu = 0.2$). Secondly, the transitions between low and high ($\mu = 0.7$) friction with the boric acid coating on Al and low and intermediate friction with the annealed boron carbide coating involved both compositional changes and redistribution of third bodies at the interface.

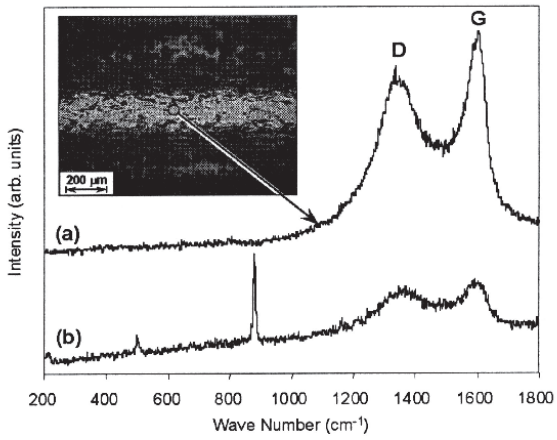

Fig. 14—*Ex situ* analysis of coating wear scar from test on annealed B_4C coating, showing Raman spectra.
(a) center of wear track
(b) as-deposited coating

With *in situ* techniques, the authors have shown that the boric acid coating on Al sustained a low friction coefficient ($\mu = 0.06$) so long as boric acid was found covering both of the contacting surfaces. Somewhat higher friction coefficients, $0.08 < \mu < 0.10$, were observed with the annealed boron carbide coating when both boric acid and carbon were in the contact. But when the boric acid disappeared and only carbon remained, the friction coefficient became $\mu = 0.20$; the latter is consistent with the friction coefficients of several forms of carbon in ambient air *(7)*, *(26)*, *(27)*, *(13)*. The friction coefficients obtained in this study also agreed with those obtained by Erdemir and co-workers *(15)* on the same coatings.

Boron carbide gave a friction coefficient ten times greater than the value obtained with the annealed boron carbide coating (see Table 1). The low friction coefficient of annealed boron carbide exposed to moist air was attributed to a surface film of boric acid by Erdemir et al. *(15)*; they also noted the existence of carbon on the annealed surfaces. The presence of both boric acid and carbon on the annealed boron carbide can be explained using thermochemical calculations (Poine). Boron carbide annealed in air at 800˚C gives

$$B_4C + O_2 \rightarrow B_2O_3 + C + CO(g)\uparrow + CO2(g)\uparrow$$

where solid carbon is favored at low partial pressures of oxygen, while at higher partial pressures the oxygen combines with carbon to form gaseous products. As discussed by Erdemir et al. *(15)*, in the presence of humidity at room temperature, the boron oxide reacts with water to form boric acid:

$$B_2O_3 + 3H_2O \rightarrow 2H_3BO_3$$

In this way, annealed B_4C exposed to humid air provides not one, but two friction-reducing compounds, boric acid and carbon.

In addition to identifying the two compounds, the *in situ* analysis demonstrated that the changes in friction coefficient correlated with the composition of third bodies in the contact. When the hemisphere broke through the boric acid coating on Al along a narrow

(Continued on next page)

(Continued from previous page)

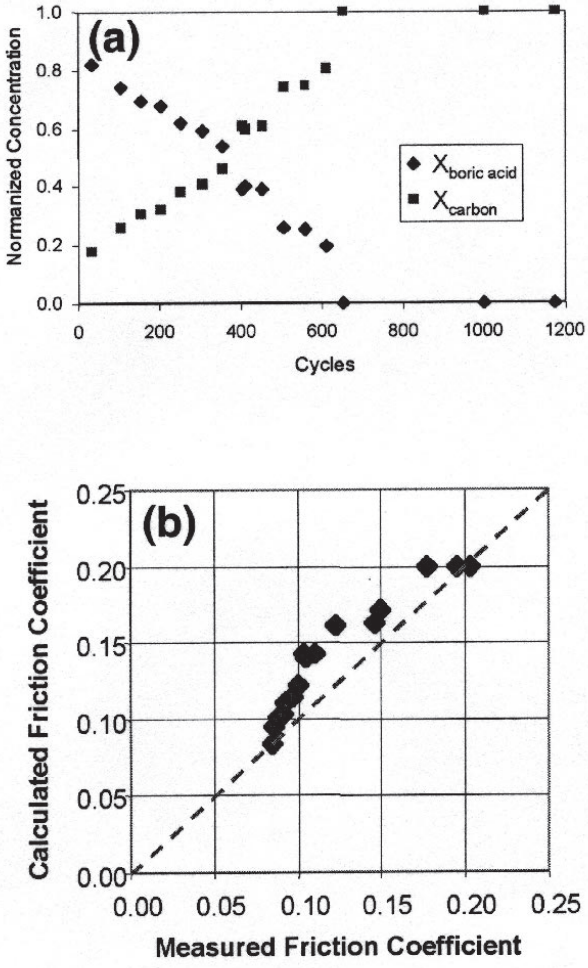

Fig. 15—(a) normalized concentrations for boric acid and carbon based on *in situ* Raman spectra
(b) a comparison of caluclated and measured friction for the test shown in Fig. 9

groove and made contact with the aluminum substrate, an Al transfer film began to adhere to the sapphire hemisphere. After breakthrough, the sapphire contact area contained two different third bodies: an ever-growing patch of metallic Al (high friction) and the remaining boric acid coating (low friction). As the friction coefficient increased from less than $\mu = 0.1$ to $\mu = 0.7$, the sliding switched from that of boric acid against itself to Al against Al *(7)*. The correlation between the friction coefficient and the computed area fraction of aluminum can be seen explicitly in Fig. 5.

This friction behavior can be expressed in terms of the rule of mixtures, written as:

$$\mu = \alpha\mu_1 + (1-\alpha)\mu_2 \qquad [1]$$

where the measured friction coefficient, μ, is the sum of contributions from each of the materials contributing to friction, and the coefficients α and $(1-\alpha)$ are taken to be the area fractions of the two materials in the sliding contact. The dashed line in Fig. 5 is a plot of Eq. [1] with $\mu_1 = 0.8$ and $\mu_2 = 0.06$. The general agreement between the data points and the dashed line supports the rule of mixtures for the two distinctly different third body transfer films. Perhaps the agreement could be improved by considering effects such as a non-uniform pressure distribution within the contact area *(4)*, but that is beyond the scope of this analysis.

In situ analysis also provided several new insights into the friction behavior of the annealed boron carbide coating, with its two lubricating compounds, boric acid and carbon. The friction coefficient during the first 400 cycles of the test, $\mu = 0.08$, was somewhat higher than that of boric acid alone, $\mu = 0.06$. This difference is probably due to having a mixture of low friction boric acid and higher friction carbon (0.2) at the sliding interface. An estimate of each can be found by substituting these friction values into Eq. [1], which gives $\alpha = 0.80$; i.e., boric acid contributed 80% to the friction coefficient and carbon, 20%.

A second insight can be seen by noticing that the friction coefficient remained relatively constant over the first 400 cycles or so (Fig. 10) even as the Raman intensity of boric acid fell to near zero (Fig. 13). This behavior is consistent with in situ observations that the velocity accommodation was interfacial sliding, i.e., low friction was controlled by boric acid at the hemisphere and track interface, and not by the bulk composition of the transfer film. Hence, only after the boric acid disappeared from the contact (and the carbon intensity increased) did the friction coefficient rise to that of carbon, $\mu \sim 0.2$. Clearly, friction was a poor predictor of the thin film lubricant depletion. However, *in situ* Raman, which monitored the amount of boric acid in the contact, was a good predictor of the lubricant depletion.

The *in situ* Raman tribometry results (Fig. 12) can be used to seek another, more quantitative, correlation between the friction behavior and the amounts of boric acid and carbon detected in the sliding contact. First we converted the normalized Raman intensities of boric acid and carbon curve in Fig. 12 to relative normalized concentrations, X, of the two components *vs*. cycles; these are plotted in Fig. 15(a). Friction coefficients were calculated by substituting the normalized concentrations – in effect α and $(1 - \alpha)$ values — into the rule of mixtures (Eq. [1]). The calculated friction coefficients are plotted against the measured friction coefficients (from Fig. 9) in Fig. 15(b). In this case, while the rule of mixtures qualitatively predicts the trend in the friction data, it is not a good fit; the calculated value overestimated the friction coefficient by as much as 30% between the two extremes. This is not surprising. First of all, the micro-Raman sampled only one small area (2 µm spot size) in the center of the contact. Since the velocity accommodation mode is mainly interfacial sliding, the authors would expect contributions from the entire width of the contact (roughly 300 µm from Fig. 10(a)) over which the composition varied. Secondly, because boric acid is a transparent material (*Handbook of Chem. and Physics*, (1970-71)), the carbon Raman contribution could have come from below boric acid at the interface, which would have overestimated the contribution of carbon to the friction coefficient calculated by Eq. [1].

The way in which the two third bodies controlled friction in the annealed boron carbide coating was very complementary: as the lower friction boric acid was worn from the contact, the carbon provided a backup solid lubricant, albeit at a higher coefficient of friction than boric acid alone. It is not clear why the slipperier material (boric acid) initially controlled friction. Perhaps it segregated to the interface, or perhaps the higher friction carbon was either buried below the interface or ejected from the contact. Nonetheless, the lower friction boric acid controlled friction when the two were present. Similarly, the use of more than one lubricant phase to maintain low friction coefficients has been exploited *(11)*, *(36)* to design

adaptive solid lubricant coatings, e.g., coatings made up of materials that are either lubricating or become lubricating during sliding. When one phase outlives its usefulness, for example, at a given temperature or in a given environment, a second lubricating phase takes over. The combination of boric acid and carbon on the surface of the annealed boron carbide coating appears to be a good example of a naturally occurring adaptive lubricant for sliding contacts in moist air.

The present experiments have also clarified the issue of how the velocity is accommodated during low friction sliding. Both *in situ* and *ex situ* analysis confirmed the presence of either boric acid or carbon on the track as well as on the hemisphere at the two steady-state friction levels, 0.06 and 0.2, respectively; this, coupled with the observation of stationary transfer films on the hemispheres, is direct evidence that interfacial sliding controlled the friction coefficient. In the transition between the two friction levels, however, a second velocity accommodation mode, recirculation of debris, became prominent. Descartes and Berthier have seen debris recirculation effects with MoS_2 coatings *(12)*, as have the authors with Pb-Mo-S coatings *(32)*. However, in the present example, it is not known if debris recirculation contributes to friction or is the effect of the increased friction due to the loss of boric acid.

Finally, the results demonstrated that an optical tribometer with a micro-Raman spectrometer could be used as a real-time monitor of the condition of sliding contacts in actual machinery. It detected changes in third bodies that were either harmful, e.g., metallic debris displacing boric acid, or beneficial, e.g., a carbon reservoir beneath the boric acid, and provided a real time measure of the loss of solid lubricant. Of course, the data could not be used for predicting performance without an understanding of the role of third bodies, and for that, further research is needed to understand the role of third bodies in controlling friction and wear.

CONCLUSIONS

In situ Raman tribometry has demonstrated that the chemistry and transport of third bodies at the interface controlled the friction coefficient and stability of two boron-containing solid lubricant coatings. Low friction ($\mu = 0.06$) was obtained by interfacial sliding between boric acid on the hemisphere and boric acid in the wear track. Slightly higher but more stable friction coefficients ($0.08 < \mu < 0.2$) were obtained with annealed boron carbide where a second solid lubricant, carbon, replaced boric acid as it wore away and carbon became the dominant third body in the sliding contact. Lubricant depletion occurred suddenly in a boric acid film on Al when a metallic Al transfer film replaced boric acid. The friction rose in proportion to the amount of Al transferred to the hemisphere. The same third-body phases were detected *in situ* and *ex situ*, which supports the validity of the more common *ex situ* analysis of wear scars in solid lubricated sliding contacts. Both Raman and optical monitoring of the contact provided advanced warning of the loss of low friction.

ACKNOWLEDGMENTS

The authors wish to thank Dr. Ali Erdemir (Argonne National Laboratory) for generously providing us with samples and useful conversations, Bob Bolster and April Coates Brabant for assistance with the design, construction and programming of the tribometer, Dr. Marc Patterson for XPS analyses, and ONR for funding the research. This research was performed while one of the authors (SDD) was at NRL on an ASEE Postdoctoral Research Fellowship.

REFERENCES

(1) Belin, M. and Martin, J. M. (1992),"Triboscopy, A New Approach to Surface Degradations of Thin Films," *Wear*, **156**, pp 151-160.

(2) Berthier, Y. and Play, D. (1982), "Wear Mechanisms in Oscillating Bearings," *Wear*, **75**, pp 369-387.

(3) Berthier, Y., Godet, M. and Brendlé, M. (1989), "Velocity Accommodation in Friction," *Trib. Trans.*, **32**, pp 490-496.

(4) Blanchet, T. A. and Sawyer, W. G. (2001),"Differential Application of Wear Models to Fractional Thin Films," *Wear*, **250**, pp 1003-1008.

(5) Blau, P. J. (1989), *Friction and Wear Transitions of Materials*, Noyes Publications, Park Ridge, NJ.

(6) Bowden, F. P. and Tabor, D. (1950), *The Friction and Lubrication of Solids*, Oxford University Press, London.

(7) Bowden, F. P. and Tabor, D. (1964), *The Friction and Lubrication of Solids, Part II*, Oxford University Press, Oxford.

(8) Buckley, D. H. (1981), *Surface Effects on Adhesion, Friction, Wear and Lubrication*, Elsevier, Amsterdam.

(9) Cann, P. M., Spikes, H. A. and Hutchinson, J. (1996), "The Development of a Spacer Layer Imaging Method (SLIM) for Mapping Elastohydrodynamic Contacts," *Trib. Trans.*, **39**, pp 915-921.

(10) Cheong, C. U. and Stair, P. C. (1998), "In Situ Study of Multialkylated Cyclopentane and Perfluoropolyalkyl Ether Chemistry in Concentrated Contacts using Ultraviolet Raman Spectroscopy," *Trib. Lett.*, **4**, pp 163-170.

(11) DellaCorte, C. and Sliney, H. E. (1987), "Composition Optimization of Self-Lubricating Chromium-Carbide-Based Composite Coatings for Use to 760ºC," *ASLE Trans.*, **30**, pp 77-83.

(12) Descartes, S. (1997), "Lubrification Solide a partir d'un revetement de MoSx: Conséquences de la rhéologie et des débits de troisième corps sur le frottement," Doctoral Thesis, INSA de Lyon, Lyon, France.

(13) Donnet, C. (1996), "Advanced Solid Lubricant Coatings for High Vacuum Environments," *Surf. Coat. Tech.*, **80**, pp 151-156.

(14) Erdemir, A. (1991), "Tribological Properties of Boric Acid and Boric-Acid-Forming Surfaces. Part II: Mechanisms of Formation and Self-Lubrication of Boric Acid Films on Boron- and Boric Oxide-Containing Surfaces," *Lubr. Eng.*, **47**, pp 179-184.

(15) Erdemir, A., Bindal, C. and Fenske, G. R. (1996), "Formation of Ultralow Friction Surface Films on Boron Carbide," *Appl. Phys. Lett.*, **68**, pp 1637-1639.

(16) Erdemir, A., Bindal, C., Zuiker, C. and Savrun, E. (1996), "Tribology of Naturally Occurring Boric Acid Films on Boron Carbide," *Surf. Coat. Tech.*, **86-87**, pp 507-510.

(17) Erdemir, A., Eryilmaz, O. L. and Fenske, G. R. (1999), "Self-Replenishing Solid Lubricant Films on Bulk Borides and Their Coatings," *Surface Engineering*, **15**, pp 291-295.

(18) Godet, M. (1984), "The Third-Body Approach: A Mechanical View of Wear," *Wear*, **100**, pp 437-452.

(19) Godet (1990), "Third-Bodies in Tribology," *Wear*, **136**, pp 29-45.

(20) Gohar, R. and Cameron, A. (1967), "The Mapping of Elastohydrodynamic Contacts," *ASLE Trans.*, **10**, pp 215-225.

(21) Handbook of Chem and Physics, 51st edition (1970-71), The Chemical Rubber Co., Cleveland, Ohio, p B74.

(22) Huong, P. V. (1991), "Structural Studies of Diamond Films and Ultrahard Materials by Raman and Micro-Raman Spectroscopies," *Diamond and Related Materials*, **1**, pp 33-41.

(23) Jullien, A., Meurisse, M. H. and Berthier, Y. (1996), "Determination of Tribological History and Wear Through Visualization in Lubricated Contacts Using a Carbon-Based Composite," *Wear*, **194**, pp 116-125.

(24) Kennedy, F. E. (1984), "Thermal and Thermomechanical Effects in Dry Sliding," *Wear*, **100**, pp 453-476.

(25) Langlade, C., Fayeulle, S. and Olier, R. (1993), "Characterization of Graphite Superficial Thin Films Achieved During Friction," *Appl. Surf. Sci.*, **65-66**, pp 83-89.

(Continued on next page)

(Continued from previous page)

(26) Miyake, S., Takahashi, S., Watanabe, I. and Yoshihara, H. (1987), "Friction and Wear Behavior of Hard Carbon Films," *ASLE Trans.*, **30**, pp 121-127.

(27) Miyoshi, K., Pouch, J. J. and Alterovitz, S. A. (1989), "Plasma-Deposited Amorphous Hydrogenated Carbon Films and Their Tribological Properties," *Mat. Sci. Forum*, **52-53**, pp 645-656.

(28) Nakamizo, M. and Tamai, K. (1984), "Raman Spectra of the Oxidized and Polished Surfaces of Carbon," *Carbon*, **22**, pp 197-198.

(29) Nakamizo, M., Kammereck, R. and Walker, P. L. (1974), "Laser Raman Studies on Carbons," *Carbon*, **12**, pp 259-267.

(30) Olsen, J. E., Fischer, T. E. and Gallois, B. (1996), "In Situ Analysis of the Tribochemical Reactions of Diamond-Like Carbon by Internal Reflection Spectroscopy," *Wear*, **200**, pp 223-237.

(31) Poine, A., *Outokumpu HSC Chemistry for Windows*, Version 3.0; Outokumpu Research Oy, Pori, Finland.

(32) Singer, I. L., Dvorak, S. D. and Wahl, K. J. (2000), "Investigation of Third Body Processes by In Vivo Raman Tribometry," in *Proc. of 9th Nordic Symp. on Tribology NORDTRIB 2000*, **1**, Andersson, P., Ronkainen, H. and Holmberg, K., eds., VTT, Espoo, Finland, pp 31-41.

(33) Singer, I. L. (1996), "Mechanics and Chemistry of Solids in Sliding Contact," *Langmuir*, **12**, pp 4486-4491.

(34) Sliney, H. E. (1977), "Dynamics of Solid Lubrication as Observed by Optical Microscopy," *ASLE Trans.*, **21**, pp 109-117.

(35) Wahl, K. J., Belin, M. and Singer, I. L. (1998), "A Triboscopic Investigation of the Wear and Friction of MoS_2 in a Reciprocating Sliding Contact," *Wear*, **214**, pp 212-220.

(36) Zabinski, J. S., Donley, M. S., Dyhouse, V. J. and McDevitt, N. T. (1992), "Chemical and Tribological Characterization of PbO-MoS_2 Films Grown by Pulsed Laser Deposition," *Thin Solid Films*, **214**, pp 156-163. ■